

ARTICLES

Ultrashort x-ray pulse propagation through resonant attenuating media

F. N. Chukhovskii, U. Teubner, and E. Förster

Max-Planck-Arbeitsgruppe "Röntgenoptik" an der Friedrich-Schiller-Universität Jena, Max-Wien-Platz 1, 07743 Jena, Germany

(Received 29 July 1996)

The propagation of ultrashort x-ray pulses through a resonant attenuating two-level atom medium is investigated on the basis of the temporal point-source (the Green-function) formalism. A general case of the small-area pulse (SAP) approximation of a traveling coherent wave is considered. The patterns of the SAP envelope $E(t, z)$ and energy $U(z)$ evolution within the medium are calculated in the cases of incident Lorentzian and exponential pulses and their dependence on the temporal *bandwidth* τ_{band} in comparison with the total dissipative relaxation time (*lifetime*) T_2 . It is shown that if τ_{band} is the same order or smaller than T_2 , the reshaping (oscillations) of the pulse envelope and/or low energy-loss effects occur in accord with the general conclusions pointed out by Crisp [Phys. Rev. A **1**, 1604 (1970)] in the case of the SAP for coherent light traveling through a resonant medium. The experimental conditions for the observation of penetration effects of the SAP of x rays are discussed. Based on the theoretical study, it is found that an ultrashort x-ray pulse emitted by an ultrashort laser-produced plasma propagates through thin resonant medium foils with low energy loss. [S0163-1829(97)05005-4]

I. INTRODUCTION

Subpicosecond high-intensity (10^{15} – 10^{18} W/cm²) lasers are capable of producing plasmas on solid targets, resulting in high intensity x-ray lines and/or continuum emission.^{1–4} The time duration τ_x of such x-ray pulses depends on the experimental conditions and ranges from subpicosecond to several tens of picoseconds.^{1,5}

The time-dependent investigations using a laser-produced plasma as a prolific source of x rays are of high interest for time-resolved photoelectron spectroscopy,⁶ probing of the dynamics of chemical reactions (see, e.g., Refs. 1 and 7), time-resolved x-ray diffraction, and in particular, measurements of lattice parameters of laser-shocked single crystals.^{8,9} These methods are adapted to the study of the mechanisms involved in shock-induced crystal surface phase transitions on sub-nanosecond timescales. Recently, the delay effects of a crystalline medium response to the time-dependent x-ray propagation were reported in Refs. 10 and 11.

The phenomenon of time-dependent x-ray interaction with a medium is of special interest by itself, if one bears in mind the well-known effects of self-induced transparency (SIT) in the coherent light optics discovered by McCall and Hahn.^{12,13} The SIT study was further developed in many subsequent papers (see, e.g., Refs. 14–18).

The SIT problem can be analyzed with the use of the inverse scattering method (ISM) developed by Zakharov and Shabat.¹⁹ Using the ISM method, Lamb¹⁶ obtained and described a whole class of special solutions to the SIT problem in terms of solitons (kinks and breathers), which undergo no energy loss during propagation in a resonant medium. In other words, the medium is completely transparent for the input pulse (decaying into solitons). Ablowitz, Kaup, and

Newell¹⁸ treated the general case, when the incident pulse decomposes into solitons, which interact with the medium without energy loss, and also yields radiation, which is absorbed by the medium. As pointed out by McCall and Hahn,¹³ solitons arise in the case of the so-called large-area pulse (LAP) approximation, whereas there is only an effect of the envelope reshaping for small-area pulses (SAP), for which the radiation energy is irreversibly transferred to the medium¹⁴ and as a result, the pulse energy is not necessarily conserved.

Recall that the pulse area $\theta(z)$ is defined as $\theta(z) \equiv \int_{-\infty}^{\infty} dt E(t, z)$ and $E(t, z) = 2\pi p \mathcal{E}(t, z) \exp(i\phi(t, z))/\hbar$, where the pulse has the form of the circular polarized wave field packet $\mathbf{E}_+(t, z) = \text{Re}[(\mathbf{i} + i\mathbf{j})\mathcal{E}(t, z)\exp(-i\Phi(t, z))]$, $\Phi(t, z) = \omega t - kz - \phi(t, z)$, traveling through a medium in the unit vector direction \mathbf{k} of increasing distance z (the unit vectors \mathbf{i} and \mathbf{j} are orthogonal to \mathbf{k} , $k = \omega/c = 2\pi/\lambda_x$; where ω , λ_x is the carrier frequency and wavelength of the radiation in vacuum, respectively; c is the speed of light, p is the dipole moment corresponding to the two-level atom transition, and \hbar is Planck's constant). Hence, the SAP approximation corresponds to $\theta(z) \ll 1$ for the pulse propagation through a resonant attenuating medium.

One example of an x-ray SAP is an x-ray line, which is emitted from an ultrashort laser-produced plasma (ULPP).^{1,4} For typical experimental parameters, the magnitude of the electric wave amplitude $|\mathcal{E}(t, 0)| \sim 50$ – 100 V cm⁻¹ (the intensity of the line at the sample position is $I_x \sim 10$ W/cm² on average, the temporal *bandwidth* τ_{band} corresponding to the spectral width of the line is equal to ~ 2 fs) and the input pulse area $\theta(0)$ can be estimated as $10^{-3} \ll 1$.

This article describes the analysis of the SAP x-ray propagation through a resonant attenuating medium. The physical and mathematical basis for the study is similar to the classi-

cal dispersion theory (see, e.g., Ref. 20) and the main results follow Crisp's approach,¹⁴ applied to the study of the SAP propagation of coherent light through matter. According to Ref. 14 as the SAP travels through a resonant medium, it excites a macroscopic polarization with a phase shift π in the input pulse for a total dissipative relaxation time (*lifetime*) T_2 after the pulse has passed. If τ_{band} drops off faster, namely: $\tau_{\text{band}} < T_2$ (the lifetime T_2 being the decay time of the macroscopic polarization), then the SAP envelope $E(t, z)$ will change sign and become negative (with respect to the input pulse) owing to the response of the medium.

In Sec. II, the problem is formulated on the basis of the reduced Maxwell equation and the explicit analytical solution of the boundary problem is derived based on the Green-function formalism. In Sec. III, the SAP shape $E(t, z)$ and energy $U(z) = 1/8\pi \int_{-\infty}^{\infty} dt |E^2(t, z)|$ evolution are considered within a resonant medium and the deviation of the z dependence of the SAP energy loss from the exponential law (Beer's law) is discussed. Some plots of the numerical evaluations of the shape and energy of the SAP propagating through resonant media are presented for the cases of Lorentzian and exponential input pulses. Finally, in Sec. IV, the physics aspects and numerical estimates for the observation of the propagation peculiarities of ultrashort x-ray pulses from ULPP through resonant attenuating media (solid foils) are discussed.

II. REDUCED MAXWELL EQUATION: SOLUTION OF BOUNDARY PROBLEM

An x-ray pulse traveling through a resonant atom medium satisfies the wave equation derived from Maxwell's equations

$$\frac{\partial^2 \mathbf{E}_+(t, z)}{\partial t^2} - c^2 \frac{\partial^2 \mathbf{E}_+(t, z)}{\partial z^2} + 4\pi \frac{\partial^2 \mathbf{P}_+(t, z)}{\partial t^2} = 0. \quad (2.1)$$

Here the resonance-induced electric dipole polarization $\mathbf{P}_+(t, z)$ can be represented as a continuum corresponding to the resultant inhomogeneously broadened two-level atomic-resonance line:^{13,17}

$$\mathbf{P}_+(t, z) = N(p/2) \int_{-\infty}^{\infty} d\gamma g(\gamma) \text{Re}[(\mathbf{i} + \mathbf{j})(u - iv) \times \exp(-i\Phi(t, z))]. \quad (2.2)$$

The function $g(\gamma)$ describes the distribution of the resonant frequencies ω_{12} at the field-carrier frequency ω , $g(\gamma) \equiv g(\omega_{12} - \omega)$ with $\int_{-\infty}^{\infty} d\gamma g(\gamma) = 1$ and $\gamma = \omega_{12} - \omega$ indicates how far an individual atomic transition frequency ω_{12} is detuned from the field-carrier frequency ω . N is the number of the radiating dipoles per unit volume. Notice that the relevant volume to be used for averaging must contain a large number of radiating dipoles (atoms) so that the induced polarization $\mathbf{P}_+(t, z)$ can be represented by a continuum according to Eq. (2.2).

The terms u and v , together with a pseudopolarization w , are identified as the electric dipole dispersion and absorption components, respectively, in accord with the following damped Bloch equations (cf. Ref. 17):

$$\dot{u} = [\gamma - \dot{\phi}(t, z)]v - u/T_2', \quad (2.3)$$

$$\dot{v} = -[\gamma - \dot{\phi}(t, z)]u + Ew - v/T_2', \quad (2.4)$$

$$\dot{w} = -Ev - [w - w_0]/T_1. \quad (2.5)$$

Here the wave-field envelope per s^{-1} $E \equiv 2\pi p \mathcal{E}/\hbar$ and the relaxation effects are taken into account phenomenologically by means of a longitudinal relaxation time T_1 and by a transverse relaxation time T_2' . The description of the x-ray pulse propagation can be obtained by solving the Maxwell equation (2.1) and Eqs. (2.2), (2.3), (2.4), and (2.5) simultaneously.

Assuming that the envelope $E(t, z)$ and phase $\phi(t, z)$ vary slowly during an optical period or over the distance of an optical wavelength, $|\partial E(\phi)/\partial t| \ll \omega |E(\phi)|$ and $|\partial E(\phi)/\partial z| \ll |E(\phi)/\lambda_x|$, one can reduce Eq. (2.1) to the scalar equation (the reduced Maxwell equation)

$$\left(\frac{\partial}{\partial t} + c \frac{\partial}{\partial z} \right) E(t, z) = 2\pi^2 i N p^2 \omega / \hbar \int_{-\infty}^{\infty} d\gamma g(\gamma) (u - iv) \exp(i\phi(t, z)). \quad (2.6)$$

The boundary condition

$$E(t) = E(t, z)|_{z=0} \quad (2.7)$$

and the initial ones

$$u(t_0, z, \gamma) = v(t_0, z, \gamma) = 0, \quad w(t_0, z, \gamma) = w(0), \quad (2.8)$$

when the time t_0 (e.g., $t_0 = -\infty$) is chosen to be immediately before the entrance of the pulse into the medium, complete the problem.

In the case of the SAP the pseudopolarization component $w(t, z, \gamma)$ of the individual atoms inside a medium does not change essentially and it can be fixed as $w(0)$ in Eqs. (2.3), (2.4), and (2.5). As a result, the SAP propagation through a medium can be described by a single linearized equation¹⁴

$$\left(\frac{\partial}{\partial t} + c \frac{\partial}{\partial z} \right) E(t, z) = -\alpha \int_0^{\infty} dt' G(t') E(t - t', z), \quad (2.9)$$

where the kernel function $G(t)$ and the constant coefficient α are defined as

$$G(t) = \exp(-t/T_2') \int_{-\infty}^{\infty} d\gamma g(\gamma) \exp(-it\gamma), \quad (2.10)$$

$$\alpha = -(2\pi^2 N p^2 \omega / \hbar) w(0) \quad (2.11)$$

($\alpha > 0$ for resonant attenuating media).

If one introduces the inverse Fourier transform

$$E(t, z) = (1/2\pi) \int_{-\infty}^{\infty} d\nu E(\nu, z) \exp(it\nu), \quad (2.12)$$

Eq. (2.9) takes the form

$$\left(i\nu + c \frac{\partial}{\partial z} + a(\nu) \right) E(\nu, z) = 0, \quad (2.13)$$

where the term $a(\nu)$ in the left-hand side of Eq. (2.13) is defined as

$$\begin{aligned} a(\nu) &= \alpha \int_0^\infty dt G(t) \exp[-i\nu t] \\ &= \alpha \int_{-\infty}^\infty d\gamma g(\gamma) / [i(\nu + \gamma) + 1/T_2']. \end{aligned} \quad (2.14)$$

Equation (2.13) can then be readily integrated

$$E(\nu, z) = E(\nu, 0) \exp[-i\nu z/c - a(\nu)z/c] \quad (2.15)$$

and the SAP solution for the complex pulse envelope (2.12) is given by the Fourier transform

$$E(t, z) = (1/2\pi) \int_{-\infty}^\infty d\nu E(\nu, 0) \exp[i\nu(t - z/c) - a(\nu)z/c]. \quad (2.16)$$

Furthermore, the distribution of the atomic frequencies is assumed to be Lorentzian around the resonant frequency deviation γ_{12}

$$g(\gamma) = (T_2^*/\pi) \{1 + [(\gamma - \gamma_{12})T_2^*]^2\}^{-1}. \quad (2.17)$$

For this particular case from Eqs. (2.14) and (2.17) one obtains

$$a(\nu) = \frac{i\alpha}{i/T_2 - \nu - \gamma_{12}}, \quad (2.18)$$

where the total transverse relaxation time T_2 is defined as

$$1/T_2 = 1/T_2' + 1/T_2^*. \quad (2.19)$$

Finally, Eq. (2.16) reduces to

$$\begin{aligned} E(t, z) &= (1/2\pi) \int_{-\infty}^\infty d\nu E(\nu, 0) \\ &\times \exp\left[i\nu(t - z/c) - \frac{i\mu_{12}z}{2[i - (\nu + \gamma_{12})T_2]} \right]. \end{aligned} \quad (2.20)$$

From Eq. (2.20) a pulse area theorem is easily deduced

$$\begin{aligned} \theta(z) &\equiv \int_{-\infty}^\infty dt E(t, z) \\ &= \theta(0) \exp\left[-\frac{\mu_{12}(\gamma_{12})z}{2} (1 - i\gamma_{12}T_2) \right], \end{aligned} \quad (2.21)$$

$$\mu_{12}(\gamma_{12}) = \frac{2\alpha T_2/c}{1 + (\gamma_{12}T_2)^2} [\mu_{12} \equiv \mu_{12}(\gamma_{12}=0)]. \quad (2.22)$$

Equations (2.20) and (2.21) immediately reduce to the corresponding expressions obtained by Crisp¹⁴ (with the exception that the effect of the resonant frequency detuning γ_{12} is taken into account) and describe the evolution of the com-

plex pulse envelope $E(t, z)$ in terms of the input pulse Fourier transform $E(\nu, 0)$, when $\gamma_{12} \neq 0$. It may be seen that the complex pulse area is exponentially damped with a decay constant $\mu_{12}(\gamma_{12})/2$ and has a linear z -dependent phase factor with a coefficient $\kappa(\gamma_{12}) = \mu_{12}(\gamma_{12})\gamma_{12}T_2/2$. Notice that the traveling pulse does not necessarily lose energy exponentially (as one will see below).

Solution (2.20), which describes the evolution of the SAP traveling through the resonant medium, can be cast into the relatively simple formula in such a way that it can be interpreted as the convolution of the time-dependent complex envelope $E(t, 0)$ of the input pulse and the temporal point-source function (the Green function) $\mathcal{G}[t]$:

$$E(t, z) = \int_{-\infty}^\infty dt' E(t', 0) \mathcal{G}[t - z/c - t'], \quad (2.23)$$

where the temporal point-source function $\mathcal{G}[t]$ is given by the following expression:

$$\mathcal{G}(t) = \exp[-i\gamma_{12}t - t/T_2] \frac{\partial}{\partial t} \{J_0[2(\mu_{12}zt/2T_2)^{1/2}] \Theta(t)\} \quad (2.24)$$

($J_0[\dots]$ is the Bessel function of the zero order, $\Theta(t)$ is the well-known step function).

Furthermore, Eqs. (2.21) and (2.23) will be used to study the SAP evolution in several cases for typical input pulses $E(t, 0)$ with the temporal bandwidth τ_{band} , namely:

- (i) delta-function pulse $E_{\text{delt}}(t, 0) = E_0 \tau_{\text{band}} \delta(t)$,
- (ii) Lorentzian pulse $E_{\text{loren}}(t, 0) = E_0 (\pi)^{-1} [1 + (t/\tau_{\text{band}})^2]^{-1}$, and
- (iii) exponential pulse $E_{\text{exp}}(t, 0) = E_0 \exp[-t/\tau_{\text{band}}] \Theta(t)$.

Basically, the most important point is the behavior of the traveling pulse energy $U(z) = 1/8\pi \int_{-\infty}^\infty dt |E^2(t, z)|$. In particular, we pose the question whether the reduction of the pulse energy does occur in accord with the usual exponential law (i.e., Beer's law) or if there are effects of the pulse interaction with the resonant medium, thus leading to an anomalous deviation from Beer's law.

III. CERTAIN PECULIARITIES OF THE SOLUTIONS

In the case of the δ -function input pulse $E_{\text{delt}}(t, 0) = E_0 \tau_{\text{band}} \delta(t)$, one readily notices from Eqs. (2.23) and (2.24) that the evolution of the traveling pulse is described by

(i)

$$\begin{aligned} E_{\text{delt}}(\tilde{t}, z) &= E_{\text{delt}}(\tilde{t}, 0) - E_0 \tau_{\text{band}} \exp[-i(\gamma_{12} - i/T_2)\tilde{t}] \\ &\times \left(\frac{\mu_{12}z}{2\tilde{t}T_2} \right)^{1/2} J_1[2(\mu_{12}z\tilde{t}/2T_2)^{1/2}] \Theta(\tilde{t}), \end{aligned} \quad (3.1)$$

where the second term on the right-hand side of Eq. (3.1) yields the medium response related to the temporal point-source pulse ($\tilde{t} = t - z/c$ is the retarded time for the pulse propagation in vacuum, $J_1[\dots]$ is the Bessel function of the first order).

Correspondingly, one can obtain the solutions for Lorentzian and exponential input pulses. Equations (2.21) and (2.23) directly yield the following expressions:

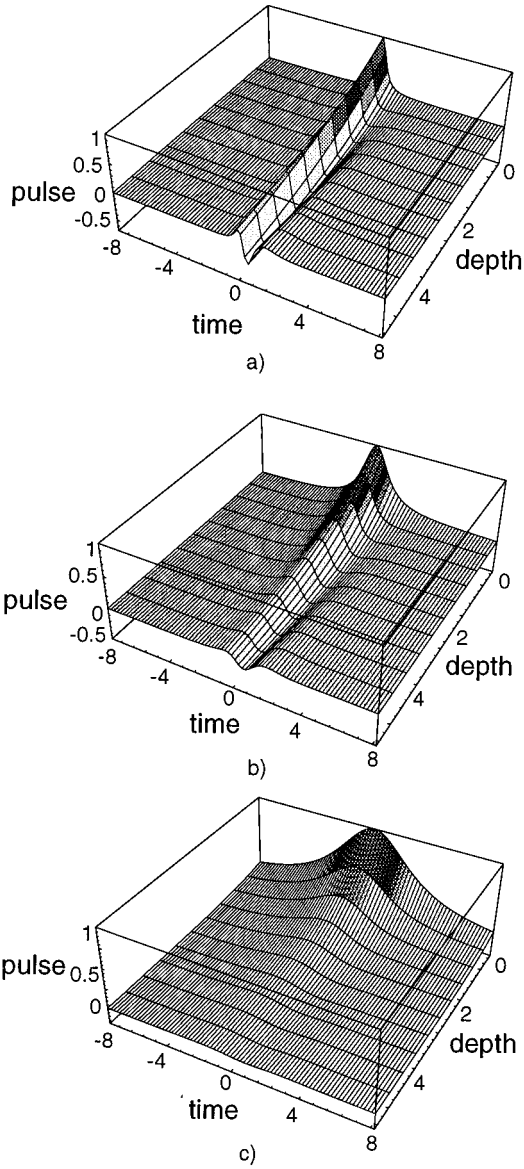


FIG. 1. Time-depth plots of the pulse (dimensionless), i.e., the electric-field envelope of an SAP that propagates through a resonant attenuating medium. The input pulse shape is a Lorentzian and (a) $\tau_{\text{band}}=1/3T_2$, (b) $\tau_{\text{band}}=T_2$, (c) $\tau_{\text{band}}=3T_2$. The time, $\tilde{t}=t-z/c$, and depth, z , are measured in units of T_2 and the double absorption length $2\mu_{12}^{-1}$, respectively.

(ii)

$$\begin{aligned}
 E_{\text{loren}}(\tilde{t}, z) = & E_{\text{loren}}(\tilde{t}, 0) - E_0 \pi^{-1} (\mu_{12} z / 2T_2)^{1/2} \\
 & \times \int_{-\infty}^{\tilde{t}} dt' [1 + (t'/\tau_{\text{band}})^2]^{-1} \\
 & \times \exp[-i(\gamma_{12} - i/T_2)(\tilde{t} - t')] \\
 & \times (\tilde{t} - t')^{-1/2} J_1\{2[\mu_{12} z (\tilde{t} - t') / 2T_2]^{1/2}\},
 \end{aligned} \tag{3.2}$$

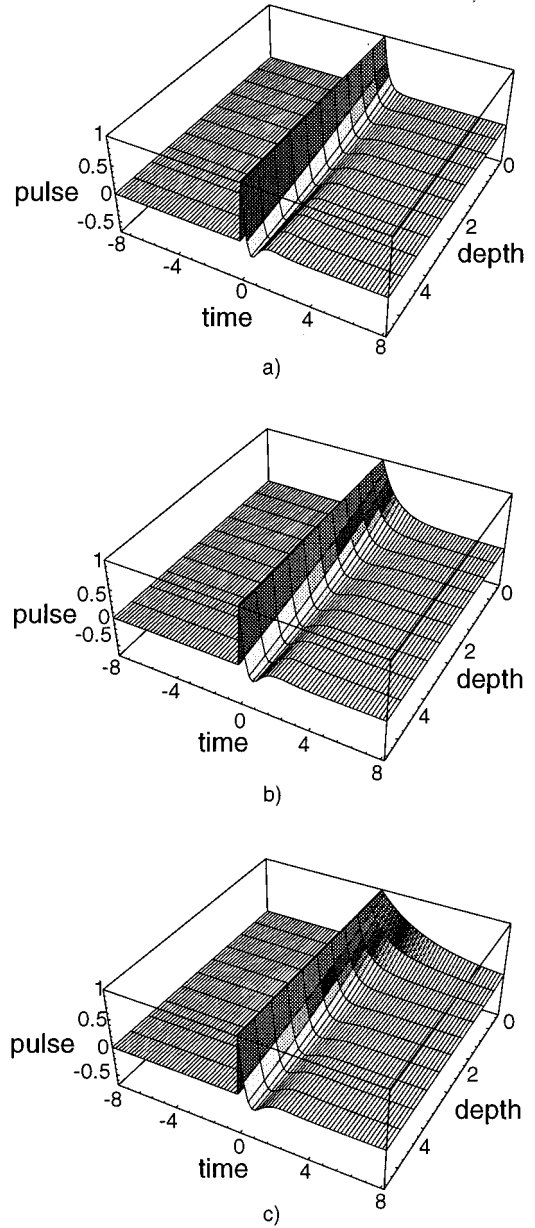


FIG. 2. Same as Fig. 1, however for an exponential input pulse.

(iii)

$$\begin{aligned}
 E_{\text{exp}}(\tilde{t}, z) = & E_{\text{exp}}(\tilde{t}, 0) - E_0 (\mu_{12} z / 2T_2)^{1/2} \Theta(\tilde{t}) \\
 & \times \int_0^{\tilde{t}} dt' \exp[-t'/\tau_{\text{band}} - i(\gamma_{12} - i/T_2)(\tilde{t} - t')] \\
 & \times (\tilde{t} - t')^{-1/2} J_1\{2[\mu_{12} z (\tilde{t} - t') / 2T_2]^{1/2}\}.
 \end{aligned} \tag{3.3}$$

The evolution of Lorentzian and exponential pulses $E(\tilde{t}, z)$ which travel through a resonant medium attenuator (i.e., $\alpha > 0$) are shown in Figs. 1 and 2 for different temporal bandwidths, τ_{band} . For simplicity it is assumed that the resonant frequency detuning $\gamma_{12} = 0$. It is seen that such pulses, in general, oscillate due to the behavior of the temporal point-source function [see Eq. (2.23)] and these oscillations are explicitly stronger when $\tau_{\text{band}} \leq T_2$. In the limit as τ_{band} goes to zero the input pulse becomes a δ function and Eqs. (3.2)

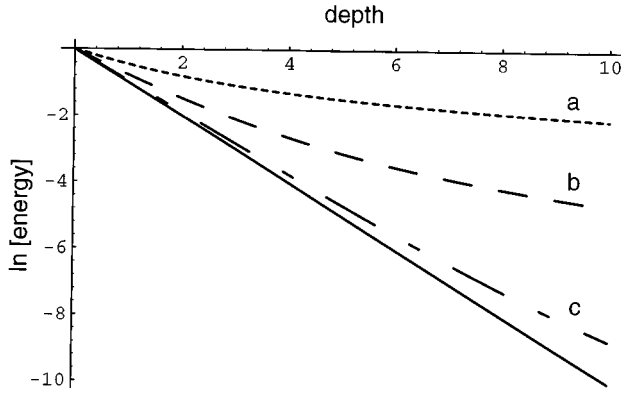


FIG. 3. Logarithm of the energy, $\ln[U(z)]$, for Lorentzian input pulses versus the depth z for the same values of the temporal bandwidth τ_{band} and the cases (a)–(c) as for Fig. 1. The depth z is measured in units of the absorption length μ_{12}^{-1} . The straight (solid) line corresponds to Beer's law.

and (3.3) transforms into Eq. (3.1). Notice that the general feature of all solutions (i)–(iii) is the first term on the right-hand sides of Eqs. (3.1), (3.2), and (3.3), which is the same as the input pulse shape $E(\tilde{t}, 0)$ and evolves in time by a simple translation $t \rightarrow \tilde{t} = t - z/c$.

With the definition of the pulse energy $U(z) = 1/8\pi \int_{-\infty}^{\infty} dt |E^2(t, z)|$ and Eqs. (2.20) and (2.22) one directly obtains

$$U(z) = (4\pi)^{-2} \int_{-\infty}^{\infty} d\nu |E^2(\nu, 0)| \exp\{-\mu_{12}(\nu + \gamma_{12})z\} \quad (3.4)$$

in terms of the product of the Fourier transform of the input envelope $E(\nu, 0)$ and the factor $\exp\{-\mu_{12}(\nu + \gamma_{12})z\}$ integrated over an entire ν region.

Correspondingly, the integrands $|E^2(\nu, 0)|$ in Eq. (3.4) have the following form:

(ii) for the Lorentzian input pulse,

$$|E_{\text{loren}}^2(\nu, 0)| = E_0^2 \tau_{\text{band}}^2 \exp[-2|\nu| \tau_{\text{band}}], \quad (3.5)$$

(iii) for the exponential input pulse,

$$|E_{\text{exp}}^2(\nu, 0)| = E_0^2 \tau_{\text{band}}^2 / (1 + \nu^2 \tau_{\text{band}}^2). \quad (3.6)$$

Then, from Eq. (3.4) it follows (for simplicity $\gamma_{12} = 0$)

(ii)

$$U_{\text{loren}}(z) = U_{\text{loren}}(0) \tau_{\text{band}} \times \int_{-\infty}^{\infty} d\nu \exp\{-2|\nu| \tau_{\text{band}} - \mu_{12}(\nu)z\}, \quad (3.7)$$

(iii)

$$U_{\text{exp}}(z) = U_{\text{exp}}(0) (\pi)^{-1} \tau_{\text{band}}$$

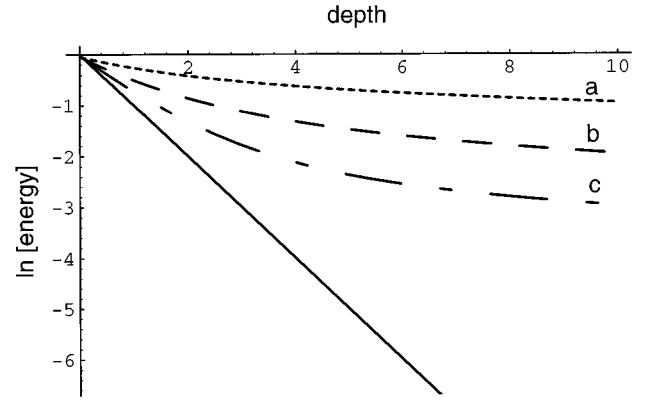


FIG. 4. Same as Fig. 3, however for an exponential input pulse.

$$\times \int_{-\infty}^{\infty} d\nu \exp\{-\mu_{12}(\nu)z\} / (1 + \nu^2 \tau_{\text{band}}^2). \quad (3.8)$$

In the case of large values ($\mu_{12}z \gg 1$) and a temporal bandwidth τ_{band} of the same order as the medium lifetime T_2 , the asymptotic energy behavior of the traveling pulses follows directly from Eqs. (3.7) and (3.8) and thus

(ii)

$$U_{\text{loren}}(z) \sim U_{\text{loren}}(0) 2\tau_{\text{band}}/T_2 K_0[4(\mu_{12}z\tau_{\text{band}}/2T_2)^{1/2}] \\ \simeq U_{\text{loren}}(0) (\pi/2)^{1/2} (\tau_{\text{band}}/T_2) (\mu_{12}z\tau_{\text{band}}/2T_2)^{-1/4} \\ \times \exp[-4(\mu_{12}z\tau_{\text{band}}/2T_2)^{1/2}], \quad (3.9)$$

($K_0[\dots]$ is the modified Bessel function of zero order),

(iii)

$$U_{\text{exp}}(z) \sim U_{\text{exp}}(0) \pi^{-1} T_2 \tau_{\text{band}}^{-1} \mu_{12}^{-2} z^{-2}. \quad (3.10)$$

The energy of Lorentzian and exponential input pulses in a resonant medium decreases with respect to Eqs. (3.9) and (3.10). The attenuation is relatively low [for example, in the case of the exponential input pulse the energy $U_{\text{exp}}(z)$ is decreasing as $\mu_{12}^{-2} z^{-2}$] and strongly differs from Beer's law, according to which $U(z)$ is decreasing as $\exp(-\mu_{12}z)$, i.e., for the absorption of a quasimonochromatic x-ray radiation with wavelength λ_{12} .

The effect of the low attenuation of the traveling pulse can be understood on the basis of Crisp's argument:¹⁴ briefly, during the SAP propagation the resonant medium "eats" the central frequencies $|\gamma| \leq 1/T_2$ of the input pulse spectrum $\Delta\gamma$ confined by $1/\tau_{\text{band}}$. The spectrum of the traveling x-ray pulse begins to resemble the superposition of two quasimonochromatic beams far off resonance, and, thus, they are weakly absorbed and provide temporal beats (see Figs. 1, 2), which become more rapid when the pulse enters into a resonant medium.

Plots of the logarithm of the pulse energy, $\ln[U(z)]$, versus the medium depth z and for comparison, the corresponding values for Beer's law are displayed in Figs. 3 and 4. The

temporal bandwidth τ_{band} (in units T_2) is given in the same values as in Figs. 1 and 2. It is seen that in the case when the temporal bandwidth τ_{band} is smaller than the medium lifetime T_2 , there are large deviations from the Beer's law and the pulse does not vanish over many "resonant" absorption lengths μ_{12}^{-1} .

IV. CONCLUSIONS AND DISCUSSION

So far special attention has been paid to illustrate the theoretical approach which allows one to construct a general solution for an arbitrary x-ray input pulse in the SAP approximation and reveal some features of its propagation through a resonant attenuating medium. Once this is done, everything else follows from Eqs. (2.21), (2.23), and (3.4) to describe the shape and depth structure of the envelope $E(t, z)$ and energy $U(z)$ for the ultrashort x-ray SAP, respectively. For the rest of this section the relevance of the previous calculations to experiments will be discussed.

In the following the ultrashort x-ray radiation from an ULPP can be regarded as the SAP. If such an x-ray pulse propagates through the resonant medium (a solid foil), the effect of the reduced energy loss is expected to be observable, when the temporal bandwidth τ_{band} is smaller than the medium lifetime T_2 .

A possible experimental scheme may be the following. The ULPP emits a broadband x-ray spectrum and the desirable x-ray line is imaged onto a sample by means of a pin-hole transmission grating spectrometer (TGS) or a grazing incidence spectrometer (see, e.g., Refs. 4 and 21), whereas all other parts of the spectrum are blocked. The detector (e.g., a CCD camera) for the observation of the transmitted x-ray line is placed directly behind the sample. The wavelength of interest λ_x has to be chosen so that it matches the two-level transition for the sample atoms (the resonant wavelength λ_{12}), in other words, $\lambda_x \approx \lambda_{12}$. An experimentally measured spectrum is presented in Fig. 5, namely the emission from an ULPP using a solid aluminum target. The absorption coefficient $\mu(\lambda_x)$ (broken line) for a carbon solid foil as the sample is shown in Fig. 5 as well.²² Some spectrum lines from specific ionization stages of an ULPP are indicated and particularly the $2p^2-2p4d$ line from AlX (i.e., an Al^{9+} ion, $\lambda_x = 4.355$ nm) can be chosen exactly to match the wavelength of the carbon K_α line, for which the experimentally measured value of λ_{12} is 4.355 nm.²³ The spectral width of the $2p^2-2p4d$ line is of the order of $\Delta\lambda_x \sim 0.02$ nm (see Fig. 5) and thus the temporal bandwidth τ_{band} may be estimated as $\tau_{\text{band}} \sim \lambda_x^2 / (\Delta\lambda_x c) \approx 3$ fs, much shorter than the typical value of the x-ray pulse duration time τ_x , which is of the order of 5–40 ps.^{1,5} Furthermore, τ_{band} is shorter than T_2 of the C K_α line being estimated as $T_2 = (\tau_{\text{rad}}^{-1} + \tau_{\text{Auger}}^{-1})^{-1} \approx \tau_{\text{Auger}} \approx 10$ fs ($\tau_{\text{rad}}, \tau_{\text{Auger}}$ is the timewidth due to the radiation and Auger electron emission, respectively),²⁴ i.e., $T_2 \approx 3\tau_{\text{band}}$.

The intensity of the input pulse, i.e., the $2p^2-2p4d$ line (and the corresponding amplitude of the electric field at the sample position), evidently depends on the experimental scheme. In the discussed case and a typical experimental geometry (e.g., typical target-TGS and TGS-sample distances are about 0.5 m) the electric field at the sample position may be estimated to be of the order of 50–100 V/cm.

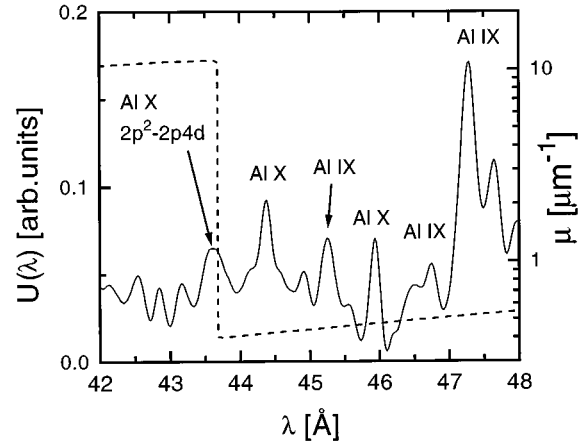


FIG. 5. Al x-ray line spectrum (solid line) in the soft x-ray region produced by a 500 fs laser pulse (laser intensity 10^{15} W/cm²). The *Bremsstrahlung* continuum (background) is subtracted. The number of photons in the x-ray lines is of the order of 10^{10} – 10^{11} photons per line per shot in 2π sr. The carbon absorption coefficient (broken line) is taken from Ref. 22.

Correspondingly, the input pulse area $\theta(0)$ is of order of $10^{-3} \ll 1$.

It is worth noting that in the discussed case, the partial "resonant" absorption length $\mu_{12}^{-1} = 0.090$ μm [equal to the difference between above and below the edge of $\mu^{-1}(\lambda_x)$ in Fig. 5], whereas the rest is "nonresonant" absorption length $\mu_{\text{rest}}^{-1} \approx 2.4$ μm , which is much larger than μ_{12}^{-1} . Thus, under the given conditions for a carbon solid foil with a thickness up to 2 μm , the effect of the reduced energy loss of the x-ray pulse is expected to be observable.

Notice that if there is a detuning between the wavelength λ_x (source) and the resonant wavelength λ_{12} (the medium transition line), calculations can be performed easily with the above equations and with the substitution [cf. Eq. (2.21)]

$$\begin{aligned} \mu_{12}(\lambda_{12}) &\rightarrow \mu_{12}(\lambda_x) \\ &= \mu_{12}(\lambda_{12}) / [1 + T_2^2 (2\pi c)^2 (\lambda_x - \lambda_{12})^2 \lambda_{12}^{-4}]. \end{aligned}$$

It is also interesting that the x-ray continuum spectrum can be used as a SAP. In this case the spectral region of interest $\Delta\lambda_x$ has to be chosen by a slit in front of the sample, which is located at a position corresponding to the wavelength λ_{12} of the sample.

Another example concerning the effect of the reduced energy loss is an x-ray SAP from an ULPP with the AlK_α emission line as source¹ and a solid Al foil as the sample. In this case the AlK_α line emitted and the AlK_α absorption line have, of course, exactly the same wavelengths, $\lambda_x = \lambda_{12} = 0.8339$ nm, and estimates, like those above, show that the effect of the reduced energy loss should be observable as well.

As shown in Sec. III the effect of envelope reshaping when the x-ray SAP propagates through the resonant attenuating medium occurs as well (cf. Figs. 1, 2). However, at the present time its observation with a time resolution on the femtosecond scale appears evidently to be rather complicated, because time-resolved x-ray pulse measurements pos-

sess a temporal resolution not better than 1–2 ps. On the other hand, the envelope reshaping effect may be hidden since the pulse duration time τ_x is much larger than the temporal bandwidth τ_{band} .

However, this obstacle can be removed, if, for instance, suprathermal electrons generated by an ULPP (Ref. 25) are used as the x-ray source, since such electrons are present only during the ultrafast laser pulse. In fact, they emit

Bremsstrahlung radiation with $\tau_x \sim \tau_{\text{band}}$,²⁶ and the condition $\tau_x \leq T_2$ possibly may be realized.

ACKNOWLEDGMENTS

We gratefully acknowledge the very fruitful discussions with P. Gibbon, G. Hölzer, and M. Schubert.

-
- ¹J. C. Kieffer and M. Chaker, *X-Ray Sci. Tech.* **4**, 312 (1994); J. C. Kieffer, Z. Jiang, A. Ikhlef, C. Y. Cote, and O. Peyrusse, *J. Opt. Soc. Am. B* **13**, 132 (1996).
- ²M. M. Murnane, H. C. Kapteyn, M. D. Rosen, and R. W. Falcone, *Science* **25**, 531 (1991).
- ³H. M. Milchberg, R. R. Freeman, S. C. Davey, and R. M. More, *Phys. Rev. Lett.* **61**, 2364 (1988); D. C. Sterns, O. L. Landen, E. M. Campbell, and J. H. Scofield, *Phys. Rev. A* **37**, 1684 (1988).
- ⁴U. Teubner, G. Kühnle, and F. P. Schäfer, *Appl. Phys. B* **54**, 493 (1992); U. Teubner, C. Wülker, W. Theobald, and E. Förster, *Phys. Plasma* **2**, 972 (1995); U. Teubner, I. Uschmann, W. Theobald, and E. Förster, *Proc. SPIE* **2270**, 106 (1996).
- ⁵U. Teubner, J. Bergmann, B. van Wonterghem, F. P. Schäfer, and R. Sauerbrey, *Phys. Rev. Lett.* **70**, 794 (1993); C. Wülker, W. Theobald, F. P. Schäfer, and J. S. Bakos, *Phys. Rev. E* **50**, 4920 (1994); J. Workman, A. Macksimchuk, X. Liu, U. Ellenberger, J. S. Coe, C. Y. Chien, and D. Umstadter, *Phys. Rev. Lett.* **75**, 2324 (1995).
- ⁶H. M. Epstein, R. L. Schwerzel, B. E. Campbell, in *Laser Interaction and Related Phenomena*, edited by H. Hora and G. H. Miley (Plenum, New York, 1984), Vol. 6, p. 149.
- ⁷J. P. Bergsma, M. H. Coladonato, P. M. Edelsten, J. D. Kahn, K. R. Wilson, and D. R. Fredkin, *J. Chem. Phys.* **84**, 6151 (1986).
- ⁸J. S. Wark, R. R. Whitlock, A. A. Hauser, J. E. Swain, and P. J. Solone, *Phys. Rev. B* **35**, 9391 (1989).
- ⁹N. C. Woolsey, J. S. Wark, and D. Riley, *J. Appl. Crystallogr.* **23**, 441 (1990).
- ¹⁰J. S. Wark and H. He, *Laser Part. Beams* **12**, 507 (1994).
- ¹¹F. N. Chukhovskii and E. Förster, *Acta Crystallogr. A* **51**, 668 (1995).
- ¹²S. L. McCall and E. L. Hahn, *Phys. Rev. Lett.* **18**, 908 (1967).
- ¹³S. L. McCall and E. L. Hahn, *Phys. Rev.* **183**, 457 (1969).
- ¹⁴M. D. Crisp, *Phys. Rev. A* **1**, 1604 (1970).
- ¹⁵G. L. Lamb, Jr., *Rev. Mod. Phys.* **43**, 99 (1971).
- ¹⁶G. L. Lamb, Jr., *Phys. Rev. Lett.* **31**, 196 (1973).
- ¹⁷L. Matulic and J. H. Eberly, *Phys. Rev. A* **6**, 822 (1972).
- ¹⁸M. J. Ablowitz, D. J. Kaup, and A. C. Newell, *J. Math. Phys.* **15**, 1852 (1974).
- ¹⁹E. V. Zacharov and A. B. Shabat, *Sov. Phys. JETP* **34**, 62 (1972).
- ²⁰L. Brillouin, *Wave Propagation and Group Velocity* (Academic, New York, 1960).
- ²¹M. Chaker, V. Bareau, J. C. Kieffer, H. Pepin, and T. W. Johnston, *Rev. Sci. Instrum.* **60**, 3386 (1989); K. Eidmann, M. Kühne, P. Müller, and G. D. Tsakiris, *J. X-Ray Sci. Technol.* **2**, 259 (1990).
- ²²B. L. Henke, E. M. Gullikson, and J. C. Davis, *At. Data Nucl. Data Tables* **54**, 202 (1993).
- ²³K. D. Sevier, *At. Data Nucl. Data Tables* **24**, 323 (1979).
- ²⁴E. M. McGuire, *Phys. Rev. A* **2**, 273 (1970); **3**, 587 (1971); **5**, 1043 (1972).
- ²⁵A. Rousse, P. Audebert, J. P. Geindre, F. Fallies, J.-C. Gauthier, A. Mysyrowicz, G. Grillon, and A. Antonetti, *Phys. Rev. E* **50**, 2200 (1994).
- ²⁶C. P. Barty, C. L. Gordon, B. E. Lemoff, C. Rose-Petruck, F. Rakis, P. M. Bell, K. R. Wilson, V. V. Yakovlev, K. Yamakawa, and G. Y. Yin, *Proc. SPIE* **2523**, 286 (1995).